

FLUID SLOSH IN A SPINNING AND OSCILLATING DISH

C.W. Hirt and R.P. Harper
Flow Science, Inc.
July 1988

OBJECTIVE

PAM-D rockets have occasionally exhibited unstable behavior during their operation. Specifically, they sometimes develop a coning motion with increasing amplitude. The reasons for such unstable behavior are not completely understood; one suggested cause is the force exerted by molten slag that collects in an annulus surrounding the exhaust nozzle. Under the action of a spinning and coning motion the slag may dynamically respond in a manner that enhances the undesirable coning behavior. Unfortunately, the slag dynamics, which involves complicated noninertial accelerations and possible nonlinear free surface motions, is difficult to analyze analytically. This has led several investigators to undertake laboratory tests of model systems in an effort to gain a better understanding of the fluid dynamic phenomena that can occur.

One such test that has been used is to replace the coning motion by a somewhat simpler motion that is easier to generate in the laboratory. A one-fifth scale model of the annulus region is arranged with its axis of symmetry oriented vertically and is given a constant spin about this axis. The table holding the apparatus is then shaken with a sinusoidal horizontal motion in one direction. Under proper conditions of spin, shaking frequency and the amount of fluid in the dish, an unusual surface wave phenomenon can be observed that induces force moments out of phase with the shaking motion.

In this note we report on two numerical calculations that were done to simulate this experimental test configuration. These calculations were intended as a demonstration of the FLOW-3D computer program. The computed results should not, therefore, be accepted as accurate until detailed comparisons have been made between the numerical and experimental data.

NUMERICAL MODEL

The FLOW-3D program is a general purpose computer program for the solution of fluid dynamics problems. Although the program has many capabilities, including both low and high speed flow analysis methods, of particular interest for the present application are its unique free surface and noninertial acceleration features. The program also has viscous stress and surface tension models, and its preprocessor makes it easy to initialize complex geometric regions.

In the calculations to be reported we used the viscous flow option, but did not use the surface tension model because it was felt that surface tension forces would be relatively small compared to inertial forces. Viscous forces are also expected to be relatively small, except near the outer radial region where the fluid depth becomes quite small.

The basic geometry consists of a shallow, approximately spherical dish with central conical and cylindrical bodies arranged axisymmetrically with the dish. For this work the fluid remains below the top of the central cylindrical obstacle so that we have only modeled an annulus region whose inner radius is the cylinder at 1.7 inch (4.318 cm) and which extends out to a radius of 3.5 inch (8.89 cm). The lowest point of the dish is assumed to define the vertical origin of the coordinate system. The total height of the region modeled is 1.0 inch (2.54 cm). We initialized the fluid free surface to a parabolic shape corresponding to a steady axial rotation rate of 1 hertz (60 rpm). Figure 1 shows the initial setup generated by the FLOW-3D preprocessor. This geometric setup, all the physical and computational parameters and the graphics requests for displaying the computed results are listed in the input data file shown in Fig. 2.

Because of the curvature of the dish, we quickly discovered that the computational mesh we first tried to use had too many cells with very small volume fractions open to flow, particularly near the outer edge of the fluid. Generally this does not cause much difficulty; but in this example, which has a large cell aspect ratio (i.e., an azimuthal cell size much larger than the radial or axial sizes), the code required an unacceptably small time step. To counter this we generated another mesh (using the code's preprocessor) that keeps the dish more or less aligned with mesh cell diagonals. This is the mesh used in Fig. 1 and shown in Fig. 3.

FLOW-3D has capabilities for general noninertial accelerations, but it is necessary for the user to supply the desired motions. Subroutine MOTION in the main program (HYDR3D)

is the place where noninertial accelerations are defined. For this application we elected to use a coordinate system fixed in the rotating dish. Thus, the motion routine must include a rotation about the z axis of 1 hertz, a gravitational acceleration in the negative z direction, and finally, horizontal accelerations corresponding to the shaking motion. In defining the latter accelerations it must be remembered that all accelerations defined in MOTION must be with respect to the rotating mesh coordinate system. For shaking in the x direction of an inertial (laboratory) frame the x and y accelerations in the rotating mesh coordinate system are,

$$x\text{-Acceleration} = A_x \cos(s)$$

$$y\text{-Acceleration} = -A_x \sin(s)$$

where s is the angle by which the mesh has rotated around the z axis and A_x is the laboratory acceleration defined as

$$A_x = a_0 \sin(\omega t) .$$

Here a_0 is the amplitude and ω is the frequency of shaking. For a purely sinusoidal shake of $\omega = 0.487$ hertz, the corresponding x direction acceleration in the rotating coordinate system is shown in Fig. 4, which is rather complex in appearance.

One further point is worth noting. Although we input the theoretically correct free surface shape, numerical approximations in the code may not be perfectly consistent with this shape and initial pressures may not be precisely the equilibrium pressures. To remedy this the code has an option that will generate an initial equilibrium configuration. We used this option to eliminate any possibility for a perturbation arising from the initial setup.

COMPUTATIONAL RESULTS

Two cases were considered. Both assumed a spin rate of 1 hertz. In the first case we used a shaking frequency of 0.487 hertz and an amplitude of 5.946 cm/s/s, which corresponds to a peak-to-peak displacement of 0.5 inch. The computed flow appeared to remain more or less in a linear range. For the second calculation we reduced the shaking frequency to 0.33 hertz and the amplitude to 1.36 cm/s/s (corresponding to a peak-to-peak displacement of 0.25 inch). This case was expected to be near resonance. These cases will be referred to as the "off resonance" and "near resonance" amplitude cases, respectively.

Off Resonance Shake

The total time computed was 10.0 s, which includes nearly 5 cycles of shaking and 10 complete rotations of the dish. Samples of the computed velocities and free surface configuration at the termination of the calculation are contained in Fig. 5.

It is quite clear from these plots that the flow is far from simple. The free surface contains waves moving both radially and circumferentially as the fluid attempts to flow back and forth around the central cylinder. Wave amplitudes generated by the shaking remain small, however, because of the relatively strong, constant gravitational and rotational accelerations.

Figure 6 shows the computed force moments about the x and y axes fixed in the dish. Figure 7 shows the result of combining the moments in the moving coordinate system into the moment about the fixed, laboratory y axis. For this figure we see that approximately two oscillations are needed for the initial transient to settle into a more or less regular oscillation. This is consistent with laboratory wave tanks in which approximately two oscillations of a wave maker are needed before a periodic wave train can be established.

Comparing the laboratory frame y moment from Fig. 7 with the laboratory x-direction acceleration, Fig. 8, we find that the two are almost exactly 180 degrees out of phase, as would be expected if the fluid is simply responding in a linear way to the shaking (i.e., a positive x acceleration produces a negative y moment). There is a small phase difference between the two plots at locations where the y moment is zero. This phase shift varies slightly, which may be a result of the numerical approximations. The average phase shift in the y moment, as measured from the plots, leads the shaking motion by about 16.5 ± 2 degrees, which is in the direction of contributing a destabilizing influence on the dynamical system.

Near Resonance Shake

In this second case we reduced the shaking amplitude to 1.36 cm/s/s for a peak-to-peak displacement of 0.25 inch, but the shaking frequency was set near resonance at 0.33 hertz.

In Fig. 9 are sample plots of velocity distributions and free-surface configurations at the end of the computational period, $t=10.0$ s. No sharp transitions in the surface profile are observed as the wave amplitudes remain relatively small. Nevertheless, it is clear that there is a complicated surface wave structure.

The computed x and y moments in the rotating frame of reference are given in Fig. 10. These moments exhibit a typical near resonance behavior. That is, initial rapid growth to a peak amplitude with a low frequency modulation.

Finally, Fig. 11 shows the resultant y moment in the stationary laboratory frame. As before, the y moment is essentially 180° out of phase with the shaking frequency, but leads the shaking frequency more than in the off resonance case. The lead is not constant, however, over the period modeled. Based on estimates made from the plot, the lead is about 64° after the first period, 39° after the second period and 18° after the third period. Because only three periods of shaking were modeled, it is unclear whether this variation in lead angle is associated with the initial startup transient or with the modulation in the y moment associated with the near resonance case. In any case, the increased phase lead near resonance is consistent with laboratory data. More work is needed, however, before detailed comparisons with the experiments can be made.

DISCUSSION

We have illustrated how FLOW-3D can be used to study nonlinear sloshing phenomena in spinning and shaking containers. The results obtained indicate that a coupled dynamic system (i.e., dish and fluid) would probably be unstable to the kind of shaking perturbation used in this study. This tentative conclusion was reached on the basis of only two example cases involving different perturbation amplitudes and frequencies but in all other respects the same. Because only two combinations of spin and shaking frequency were studied, however, our conclusion must not be taken as proven in any definitive sense.

These calculations provide an illustration of some possibilities for using FLOW-3D to investigate complicated free-surface fluid dynamics. In view of the general formulation of the code to treat any noninertial acceleration, it is possible to replace the simple unidirectional shaking in the laboratory frame with a motion corresponding to a precession of the spinning PAM-D rocket with axial acceleration. The code also has a surface tension model so that these surface forces could be included in further studies. (The code's wall adhesion feature, however, may not work accurately enough in this case because of the shallow angle between the fluid and wall.)

It would be desirable in future calculations to increase the mesh resolution, especially in the azimuthal direction. It would

additionally be interesting to explore other spin and shaking frequency combinations. Clearly, there are many directions in which these preliminary calculations can be expanded. In particular, more calculations should be undertaken and compared directly with experimental data in order to establish a validation base for FLOW-3D in this application area.

COMPUTATIONAL REQUIREMENTS

All calculations reported here were performed with code version FLOW-3D/88 running on a MicroVAX II computer. This is not a particularly fast machine, but it does support a virtual memory that makes three-dimensional calculations possible. The off resonance example required approximately 20.38 CPU hours to cover 10.0 s of real time (not quite 5 cycles of the perturbation). The near resonance case required 31.47 CPU hours for the same amount of real time. These may seem like long computing times, but considering the amount of detail produced and the fact that the MicroVAX is not a large, expensive machine, the cost-to-benefit ratio is quite low. Newer low cost computers, for instance the new SUN workstation, should reduce these CPU times to approximately 5 hours and 8 hours, respectively (based on FLOW-3D comparison speeds).

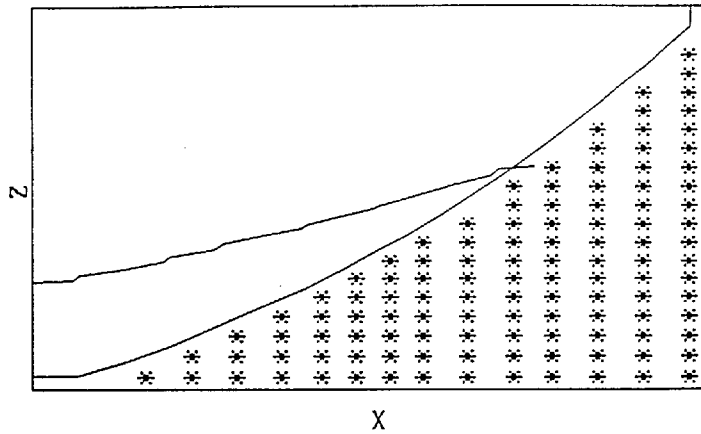


Fig. 1. Computational setup for PAMD model calculations. Axis of rotational symmetry is 4.318 cm left of the left plot edge.

```

PAM D SLAG
$XFUT
  MUI=.0068,      IWSH=1,      AVRCK=-2.1,
  ISS=1,          IADIZ=1,      OMEGA=1.2,
  ITB=1,          SPIN=6.283,   A0=5.946,
  OMG0=3.06,     GZ=-980.,     WF=4,
  IPDIS=1,       TWFIN=10.0,   WBK=4,
  RHOF=1.7,      IACCF=1,      CYL=1.0,
  PLTDT=2.0,     HPLTDT=0.05, SPRTDT=0.05,
  PRTDT=2.0,     ITMAX=100,    JFPR=12,
  ILPR=12,       IRPR=15,      KTPR=16,
  JBKPR=20,      KBPR=13,      WT=2,
  WL=2,          WR=2,
  WB=2,
$END
$SMESH
  NXCELT=16,     SIZEX(2)=.3048,  SIZEX(8)=.3048,
  PX(1)=4.318,   PX(2)=6.1468,   PX(3)=6.40,
  PX(4)=6.625,   PX(5)=6.85,     PX(6)=7.0612,
  PX(7)=7.45,    PX(8)=7.9756,   PX(9)=8.89,
  NYCELT=18,     PY(2)=55.858,
  NZCELT=20,     PZ(2)=0.2807,   PZ(3)=0.6565,
  PZ(4)=1.1392,  PZ(5)=1.747,    PZ(6)=2.509,
$END
$OBS
  NOBS=1,
  CX2(1)=-1.0,   CY2(1)=-1.0,    CZ2(1)=-1.0,
  CRXY(1)=3.353, CZ(1)=20.462,   CC(1)=4.1648,
  XL(1)=-20.0,
$END
$FL
  NFLS=1,        FLHT=0.8,
  FCZ(1)=1.0,    FCC(1)=-0.325,  FCX2(1)=-0.0201,
  FCY2(1)=-0.0201, FXL(1)=-20.0,
$END
$BF
$END
$TEMP
$END
$GRAFIC
  NVPLTS=4,      NSPLTS=1,       NWINF=1,
  JV1(1)=11,     JV2(1)=11,      IV1(2)=6,
  IV2(2)=6,      IV1(3)=10,     IV2(3)=10,
  JV2(4)=2,
  XEA(1)=30.0,   YEA(1)=0.0,     ZEA(1)=10.0,
$END
$PARTS
$END

```

Fig. 2. Input data file for lower amplitude case.

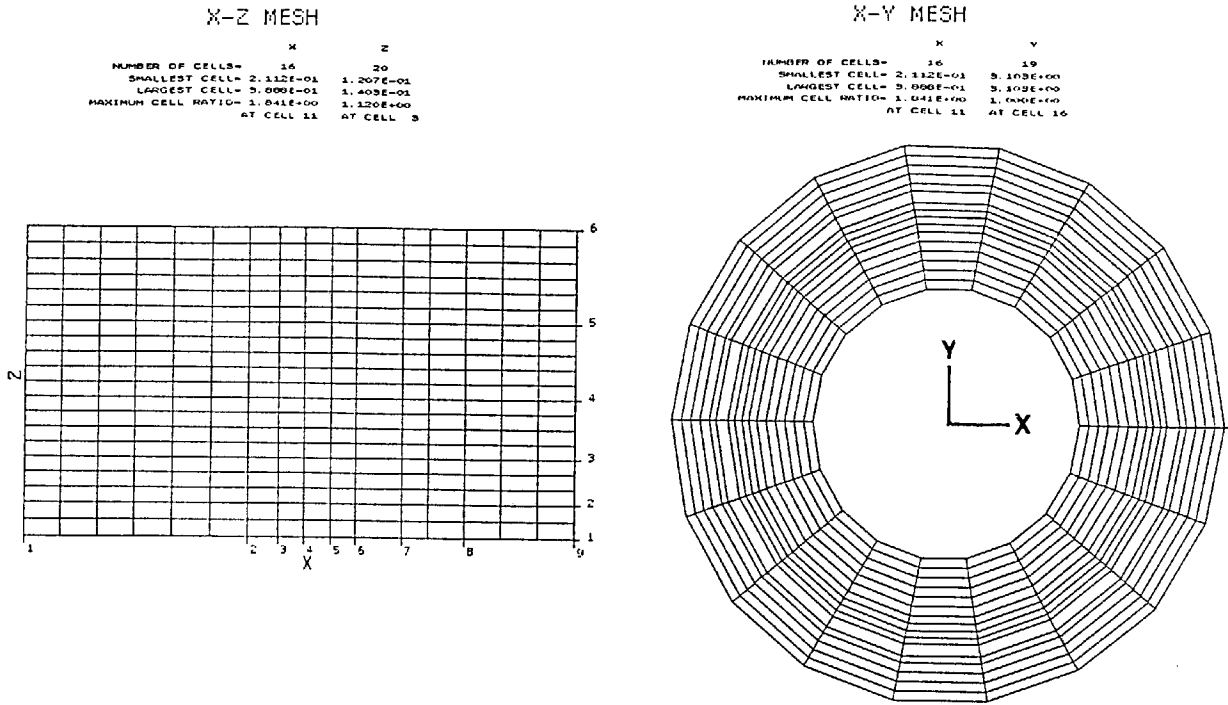


Fig. 3. Computational mesh used for all calculations.

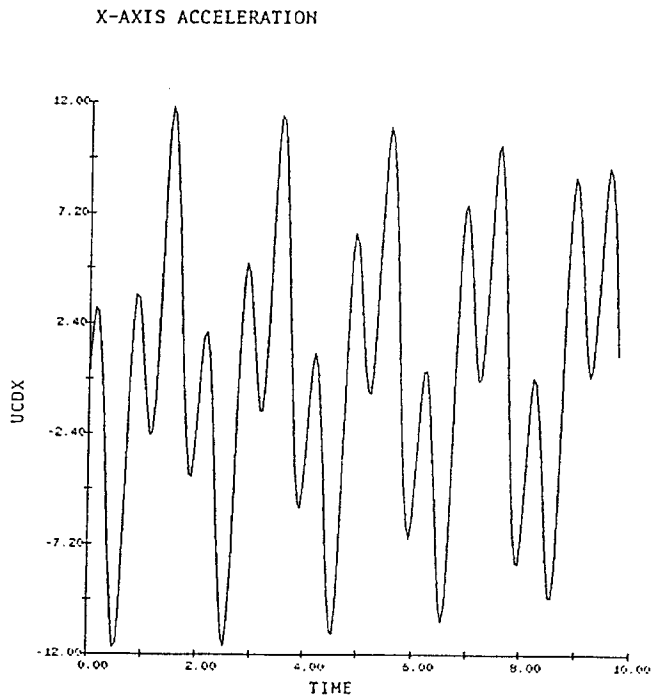


Fig. 4. Time history of perturbing x acceleration in frame of reference rotating with the dish.

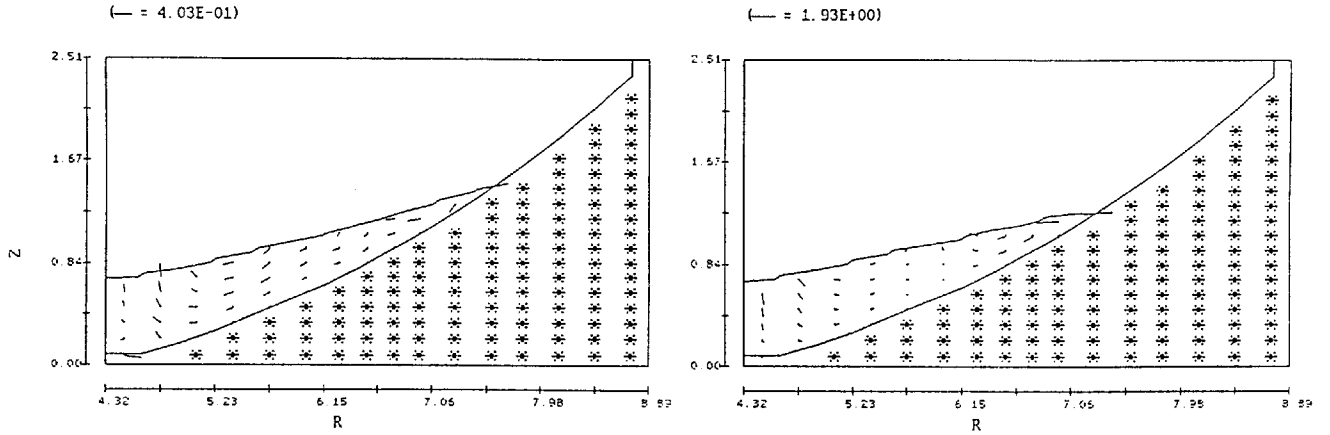


Fig. 5. Computed velocity field in $\theta = 0^\circ$ (left) and $\theta = 180^\circ$ (right) planes.

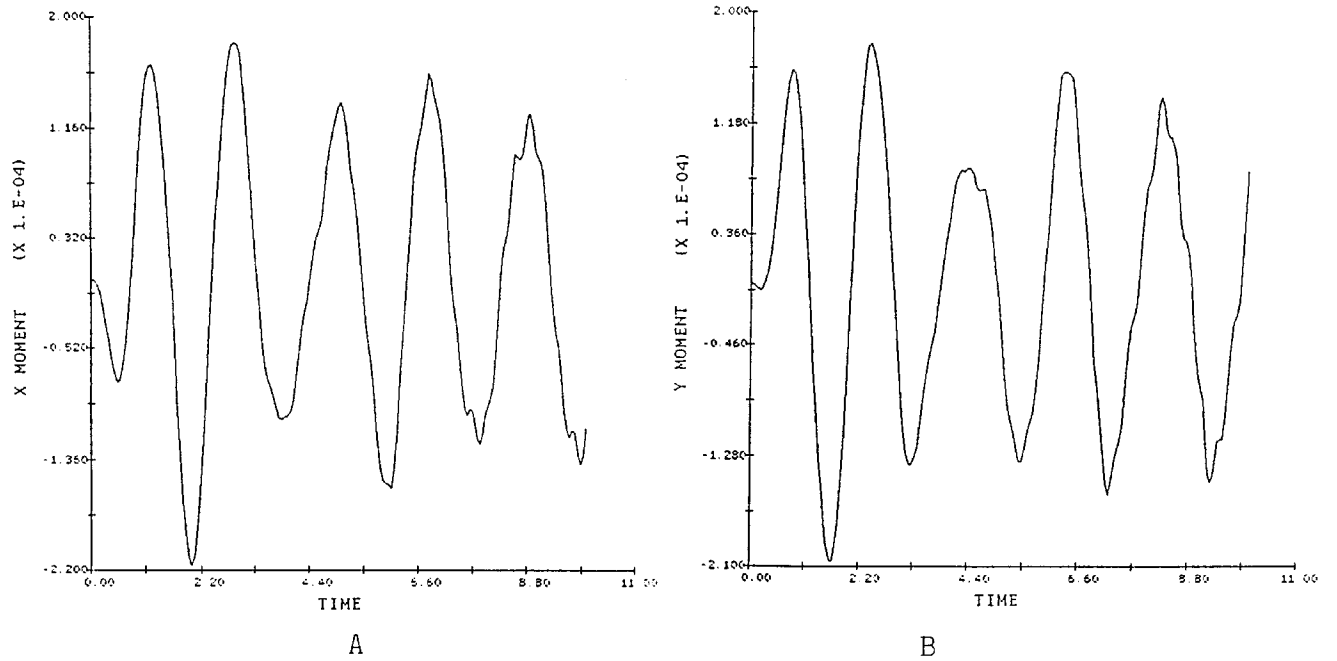


Fig. 6. Computed x-moment history (A) and y-moment history (B) with respect to rotating coordinate system.

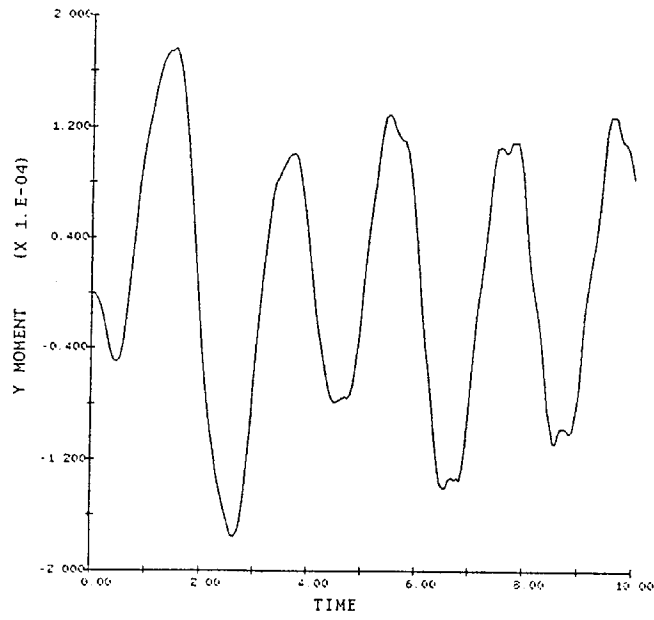


Fig. 7. Computed y-moment history with respect to laboratory frame.

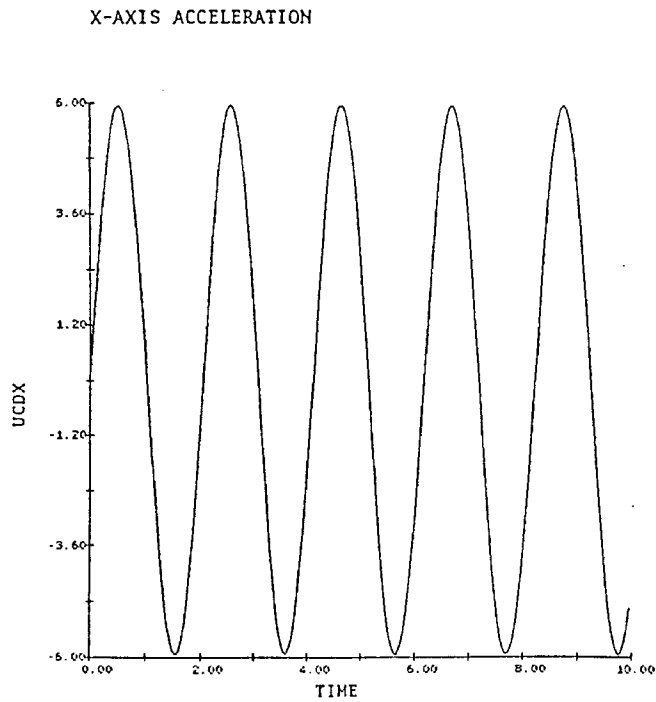


Fig. 8. Perturbation acceleration history in laboratory x direction.

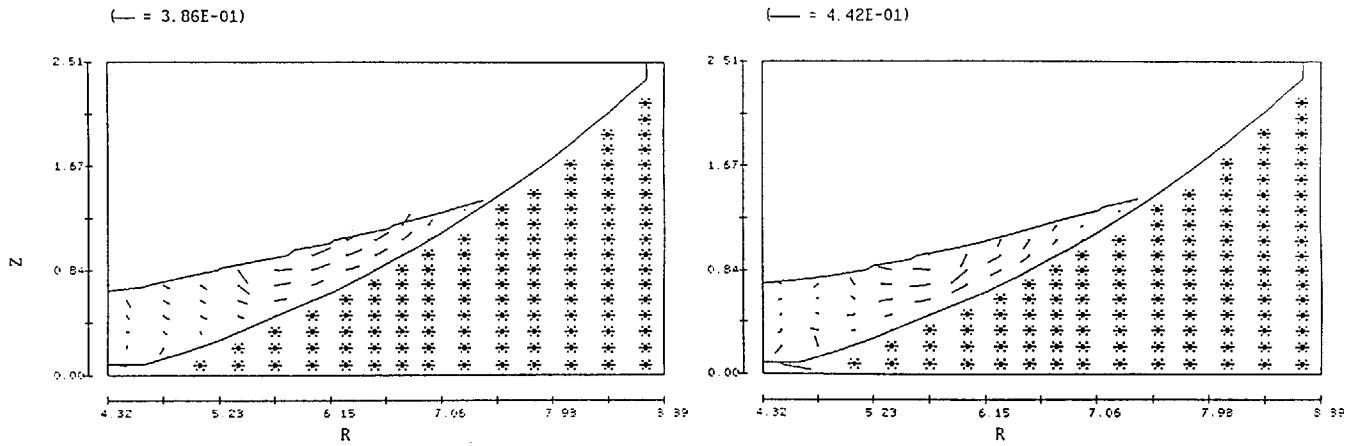


Fig. 9A. Near resonance velocities and free surface location in constant theta = 0° (left) and theta = 180° (right) planes at $t = 10.0$ s.

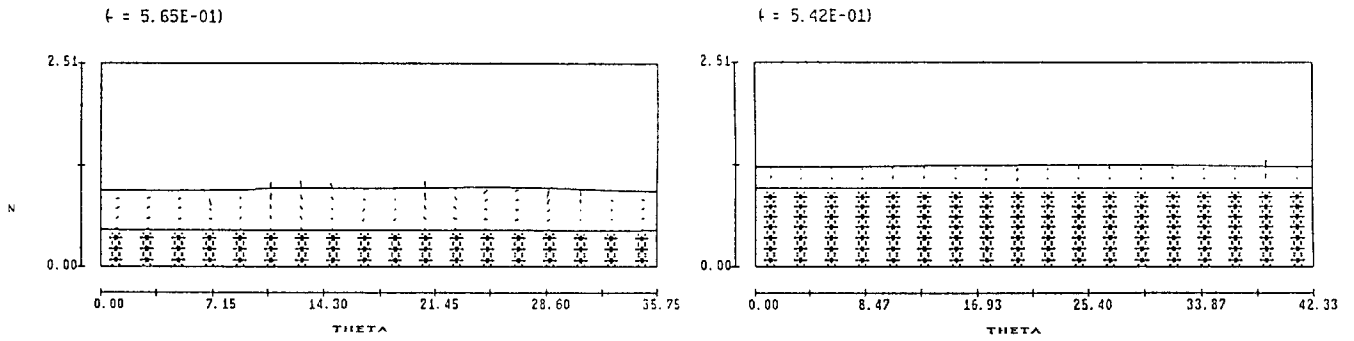


Fig. 9B. Near resonance velocities and free surface location in constant radial planes $r = 5.69$ (left) and $r = 6.74$ (right). Vertical scale has been amplified.

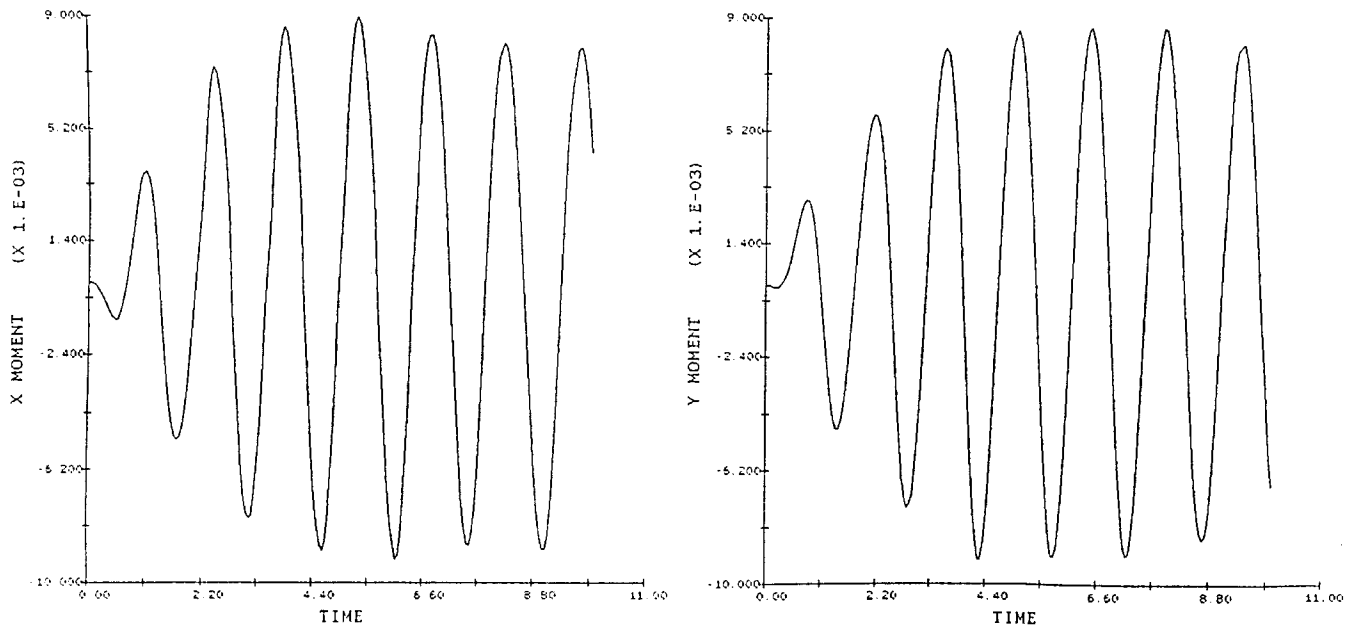


Fig. 10. Computed histories for x moment (left) and y moment (right) in rotating coordinate frame for near resonance case.

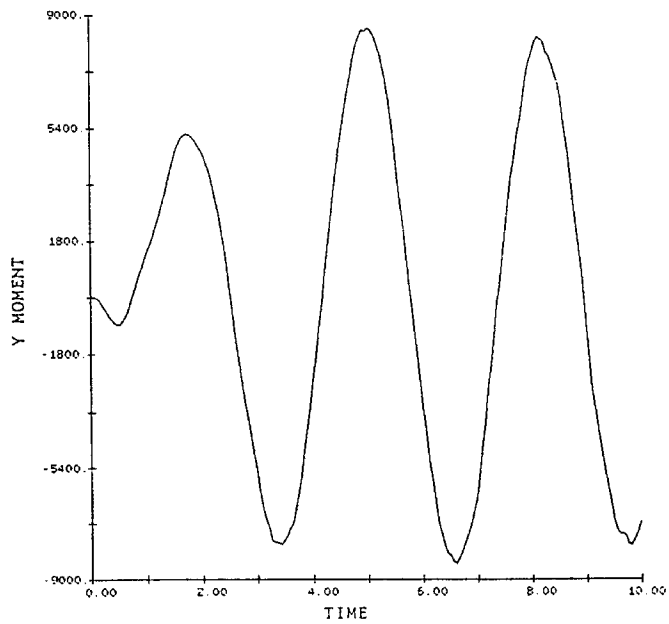


Fig. 11. Y moment history in fixed laboratory frame for near resonance case.